Journal of Paleontology, 88(4), 2014, p. 735–746

0022-3360/14/0088-735$03.00
DOI: 10.1666/13-088

THE WALKING DEAD: BLENDER AS A TOOL FOR PALEONTOLOGISTS WITH A CASE STUDY ON EXTINCT ARACHNIDS

RUSSELL GARWOOD[1] AND JASON DUNLOP[2]

[1]School of Earth, Atmospheric and Environmental Sciences and The Manchester X-Ray Imaging Facility, School of Materials, University of Manchester, Manchester, M13 9PL, UK, <russell.garwood@manchester.ac.uk>; and [2]Museum für Naturkunde, Leibniz Institute for Research on Evolution and Biodiversity at the Humboldt University Berlin, D-10115 Berlin, Germany, <Jason.Dunlop@mfn-berlin.de>

ABSTRACT—This paper serves two roles. First, it acts as an introduction to Blender, an open-source computer graphics program, which can be of utility to paleontologists. To lessen the software's otherwise steep learning curve, a step-by-step guide to create an idealized reconstruction of a fossil in the form of a three-dimensional model in Blender, or to use the software to render results from 'virtual paleontology' techniques, is provided as an online supplemental data file. Second, here we demonstrate the use of Blender with a case study on the extinct trigonotarbid arachnids. We report the limb articulations of members of the Devonian genus *Palaeocharinus* on the basis of exceptionally preserved fossils from the Rhynie Cherts of Scotland. We use these newly reported articulations to create a Blender model, and draw comparisons with the gait of extant arachnids to produce as accurate a representation of the trigonotarbid flexing its limbs and walking as possible, presented in additional online supplemental data files. Knowledge of the limb articulations of trigonotarbid arachnids also allows us to discuss their functional morphology: trigonotarbids' limbs and gait were likely comparable to extant cursorial spiders, but lacked some innovations seen in more derived arachnids.

INTRODUCTION

BLENDER (BLENDER.ORG) is an open source, freely available, and cross-platform 3-D computer graphics application maintained and developed by The Blender Foundation. It is versatile, allowing users to create, import, and modify 3-D objects, then light, color and texture, and finally raytrace the resulting models. It also provides the ability to animate 3-D objects, and edit videos, in addition to many more complex options geared towards detailed, photo-realistic raytracing which are beyond the scope of most paleontological applications. Blender was first released under a GNU license in 2002 and over the last decade has developed two primary capacities in the paleontological community. A number of authors have used Blender to manually model meshes, creating raytraced, idealized reconstructions of fossil organisms (Stein, 2010; Haug et al., 2011, 2012; Stein and Selden, 2012; Haug and Haug, 2012; see also Background discussion below). By contrast, others have used Blender as a means to produce high-quality figures for publication of CT-scanned data, following processing with other software suites (Garwood and Sutton, 2010, 2012; Garwood et al., 2011, 2012; Spencer et al., 2012; Zamora et al., 2012; Giles and Friedman, 2013). Despite increasing applications within the paleontological community, and recognition of the utility of 3-D reconstruction in all its forms (Sutton, 2008; Garwood et al., 2010), 3-D software—and arguably Blender in particular—has a very steep learning curve. No guides exist for the application of Blender in the scientific sphere.

Here we present a study completed with the assistance of Blender in which we demonstrate the value and applicability of the software, coupled with an introductory tutorial (online Supplemental Data file 1). This is intended to provide an accessible, step-by-step guide to using Blender, assumes limited computational background knowledge, and is aimed at practicing paleontologists who are considering using Blender for their publications. We focus on an extinct group of arachnids called the trigonotarbids as our model organism, for which there are a number of well-preserved and three-dimensional fossils from the Scottish Rhynie and Windyfield cherts that document their limb anatomy in some detail (e.g., Dunlop et al., 2009; see also below). This facilitates an accurate and reliable reconstruction of the limb articulations, and through comparison with morphology (Shultz, 1989) and walking gaits in modern arachnids (Wilson, 1967; Ward and Humphreys, 1981; Shultz, 1987; Biancardi et al., 2011; Spagna and Peattie, 2012) we have created an animated Blender model that we hope yields a realistic impression of how these Paleozoic animals may have walked in life.

BACKGROUND

Trigonotarbids.—Members of the extinct arachnid order Trigonotarbida superficially resemble spiders, but possessed nine opisthosomal tergites divided into median and lateral plates, and lacked silk-producing spinnerets (Garwood et al., 2009; Poschmann and Dunlop, 2011). Trigonotarbids are found among the earliest terrestrial animal communities, dating back to the late Silurian (Přídolí; Dunlop, 1996), and were thus probably amongst the first predators on land. Numerous Devonian fossils also exist, including three-dimensional specimens from the Rhynie and Windyfield Cherts of Scotland (see below), as well as other more conventional impression fossils from Alken an der Mosel in Germany (Poschmann and Dunlop, 2010), and some adjacent localities, and Tredomen in Wales (Dunlop and Selden, 2004). More than sixty trigonotarbid species are known though this is likely to be an overestimate of their diversity. Authors such as Frič (1904) and Petrunkevitch (1949, 1953) erected genera and species on the basis of superficial, often preservational, differences (Shear, 2000). Revisions have usually resulted in the recognition of numerous synonyms (e.g., Garwood and Dunlop, 2011). Nevertheless, the fossil record does suggests a peak of diversity during the Upper Carboniferous (Dunlop and Rößler, 2013, table 1; Garwood et al., 2009; Hyžný et al., 2013). During this period, numerous families developed heavy spines and dense dorsal tuberculation (Dunlop and Garwood, in press), and increased the structural complexity of their carapace. Some may have practiced ambush predation (Garwood and Dunlop, 2011). The youngest trigonotarbids date from the Lower Permian

(Asselian and Sakmarian) and the cause of their eventual extinction remains unclear (reviewed by Dunlop and Rößler, 2013). Factors may include climate change and loss of the coal swamps, tetrapod predation, and competition from other arthropods such as spiders.

Trigonotarbid anatomy (both external and internal) is known in considerable detail, thanks largely to the exceptionally preserved chert specimens noted above. For further accounts of these fossils from the Early Devonian of Scotland see also Hirst (1923), Hirst and Maulik (1926), Shear et al. (1987), and Fayers et al. (2005). This remarkable material also yields internal details of both the foregut (Dunlop, 1994a) and the lungs (Claridge and Lyon 1961; Kamenz et al., 2008). Of particular relevance to the present project is the preservation of external limb articulations, or condyles, as darkened thickenings of the cuticle on the pedipalps and legs. In rare cases even sclerotized internal muscle tendons can be resolved—as figured for the pedipalp by Dunlop et al. (2009, fig. 3d, 3f)—offering insights into the animal's musculature. However, corresponding details from the walking legs were only previously figured in the unpublished thesis of Dunlop (1994b). We formally publish these observations here, and use a Rhynie trigonotarbid as a model organism for creating a Blender reconstruction with correct limb articulations. This enables an animation showing a pattern of anatomically accurate limb flexion.

Meshes and raytracing.—A limited knowledge of the computational aspects of 3-D reconstruction will be beneficial to this introduction. As previously outlined, Blender has two primary applications in paleontology: 1) mesh creation and 2) the high-quality rendering of surfaces. The latter can be derived from tomography datasets through processing in a suitable software package (e.g., Avizo, VGStudio Max, Drishti or SPIERS) (for a full overview we direct the reader to Abel, 2012), or from surfaces captured directly using, for example, photogrammetry or laser scanning. Whatever the source, Blender uses a raytracing algorithm to render images from surface geometries. These three-dimensional polygon meshes allow the surface topology of an object to be modeled through a series of interconnected triangles, each of which is defined by three points in space.

If creating an idealized reconstruction of a taxon from multiple flattened fossils, or a variety of cross-sectional profiles through samples, Blender allows the user to manually create and then modify meshes, which can consequently be rendered from multiple angles or in animations for publications. This is usually achieved through the insertion of so-called 'mesh primitives' in the software (such as tubes and cubes) and the subsequent modification of these through both manual editing and the use of modifiers, i.e., operations which edit the mesh. This is known as box-modeling (see online Supplemental Data file 1 for a more detailed outline). If, by contrast, data acquired through another technique needs to be rendered, the vast majority of methodologies for the 3-D digitization of fossils will include the creation of meshes prior to visualization (see further discussion in Sutton et al., 2012). These can be exported from other software and imported into Blender. Although some of these datasets will comprise multiple objects, and can have very high triangle counts—especially noisy CT data—Blender can successfully import all but the largest meshes, and a wide range of file formats. For example, in tests for the current publication, a six-yr-old PC (12 GB RAM, NVIDIA GeForce GTX 280 graphics card) could load a mesh of 50 million triangles, and an ultrabook (4 GB RAM, integrated Intel Graphics) could load 10 million. We note here as a reminder, however, that another piece of software (e.g., Avizo, Amira, Mimics, SPIERS) is typically required to prepare data and convert to an appropriate mesh format.

Blender uses a raytracing algorithm to render meshes, an approach which allows highly realistic shadow and lighting effects to be created (Whitted, 1980). This works by modeling the path of light rays backwards from an imaginary camera or eye, through each pixel in a virtual screen (Arvo, 1986). Each of these rays is then tested for intersection with the objects to be rendered in a scene. The nearest object is identified, and the incoming light at this point is combined with the material's texture and properties, after which the correct color for a given pixel can be calculated. If the object is reflective or refractive, further rays are cast into the scene, and the pixel color can be updated (Cook et al., 1984). This is repeated until a maximum number of reflections or maximum distance without intersection is achieved.

METHODS

Fossils.—The Rhynie Chert fossils forming the basis of the present reconstruction can all be assigned to the genus *Palaeocharinus* Hirst, 1923 (Arachnida, Trigonotarbida, Palaeocharinidae) and are held in the Natural History Museum, London (NHM). The material is currently assigned to a range of species, most of which are probably synonyms (see comments in the unpublished thesis of Dunlop, 1994b). Pending formal revision, we prefer to pool this anatomically homogenous material as *Palaeocharinus* spp. Specimens In 24671, In 24673, In 27752, In 27756–58 and In 27760 proved to be particularly useful in resolving the position of limb condyles (see also Fig. 1.1–1.16). All fossils consist of slide-mounted chert fragments or thin sections. The fragments were studied using a Leica MZ16A stereomicroscope with both incident and transmitted light. The latter proved more suitable for understanding the three-dimensional anatomy of Rhynie Chert material in translucent fragments such as the limbs presented herein. The software CombineZM was used to create the panels (Fig. 1) by combining photographs taken at multiple focal depths (see Bercovici et al., 2009). Slide-mounted thin sections of chert were examined using a biological microscope. In a wider context, the Rhynie and adjacent Windyfield Chert is a world-famous fossil locality found in Aberdeenshire, Scotland, U.K. These are a silicified sinter deposits lain down in a hot springs environment, conventionally dated to the Lower Devonian (Pragian) of about 410 Ma (Parry et al., 2011). For details of the geological setting and general biota see Rice et al. (2002) and Fayers and Trewin (2004). These localities represent one of the oldest terrestrial ecosystems, and thus the fossil arachnids reconstructed here would have been among the oldest animals—and one of the first predators—to walk on land.

Blender.—Online Supplemental Data file 1 provides a general introduction to Blender. To accompany this, here we provide a more detailed workflow, outlining the creation of the paleocharinid model presented herein. The only three-dimensionally preserved paleocharinid taxa are from the Rhynie and Windyfield Cherts, a deposit that is not conducive to analysis with CT. Accordingly no meshes of paleocharinids exist, requiring one to be created for the present study. When building reconstructions, recycling is a valuable approach, and in the present study the body of an anthracomartid trigonotarbid—a family which is probably closely related to palaeocharinids—was imported from an existing STL file. Anthracomartids are similar in prosomal morphology to paleocharinids. The model of the former could thus be used as a basis for reconstructing the prosomal morphology of the latter through manual editing of the mesh to approach the anatomy seen in the Rhynie and Windyfield Chert fossils. In addition to saving time during modeling, this is included here to demonstrate the utility of Blender's import functions. We used the species *Anthracomartus hindi* Pocock, 1911, herein. This was presented in Garwood and Dunlop (2011), wherein a tomographic dataset was surfaced with SPIERS (see

https://doi.org/10.1666/13-088 Published online by Cambridge University Press

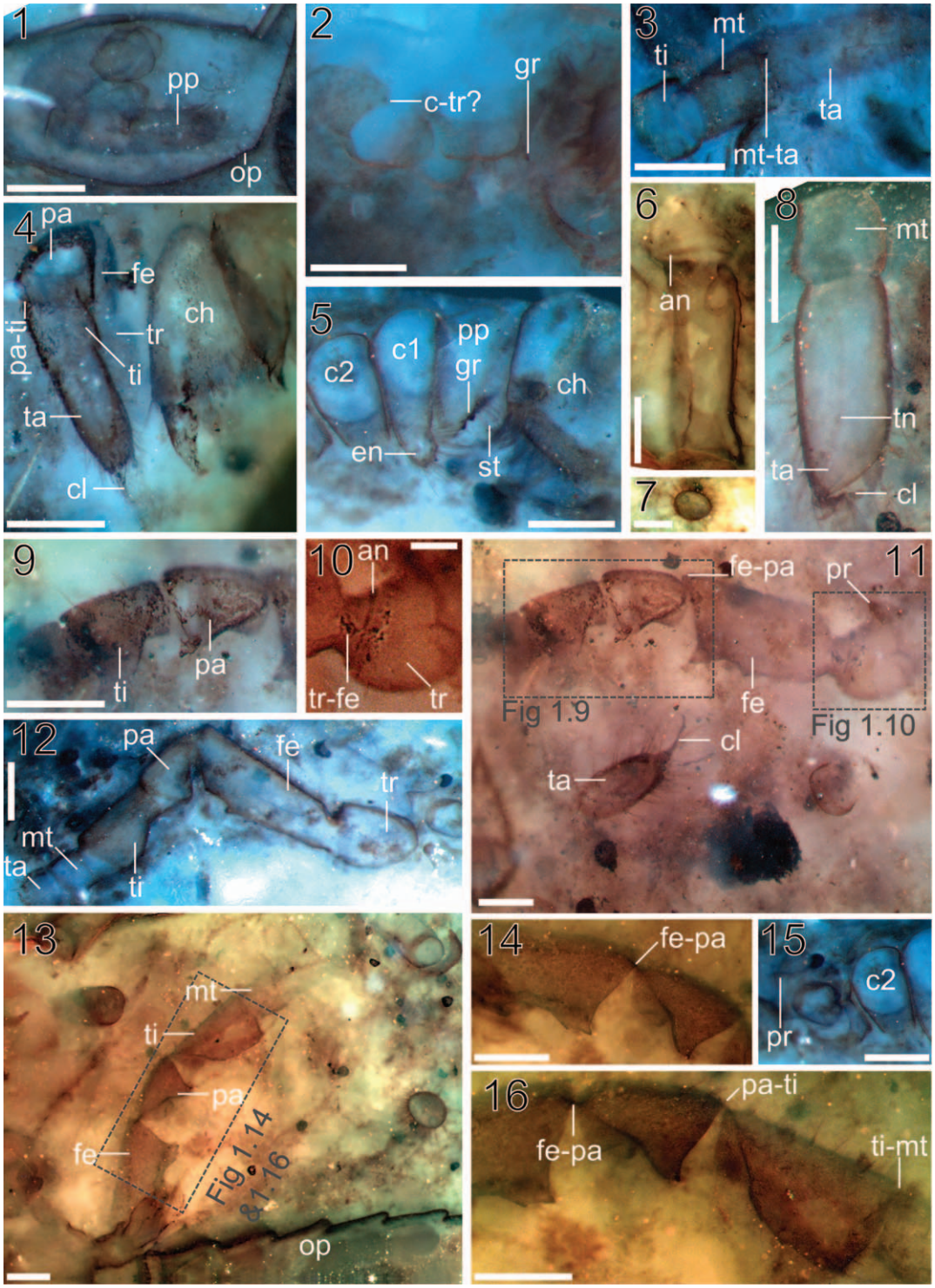

FIGURE *1*—Limbs of *Palaeocharinus* spp. from the Early Devonian Rhynie Chert of Scotland. *1*, transverse section of an opisthosoma containing an articulated pedipalp, palaeocharinid NHM In 24685; *2,* a chelicera, palpal and leg coxae in section, showing granules on the palpal coxae, *P. calmani* Hirst, 1923, holotype, NHM In 24675; *3*, tibia, metatarsus and tarsus, showing metarsus-tarsus articulation as a dark spike of cuticle, *Palaeocharinus* sp. NHM In 27760; *4*, details of the chelicerae and pedipalp, including the patella-tibia articulation and majority of the pedpalp podomeres, *P. rhyniensis* Hirst, 1923 NHM In 24673, holotype; *5*, chelicerae, and proximal pedipalp and walking legs, showing palpal coxal granulation and setae, *Palaeocharinus* sp. NHM RC/080; *6*, trochanter and femur showing annulus, *Palaeocharinus* sp. NHM In 24685; *7*, cross-section of a limb, *P. scourfieldi* Hirst, 1923, NHM In 27756; *8*, metatarsus and tarsus of a walking limb, demonstrating the base of the terminal claws and an internal tendon running up from the claw base, *Palaeocharinus* sp. NHM In 27758, *9*, tibia and patella of a walking limb, *P. rhyniensis* NHM In 24673; *10*, detail of trochanter of walking limb, *P. rhyniensis* NHM In 24673; *11*, almost complete walking limb, *P. rhyniensis* NHM In 24673; *12*, complete limb in section, *Palaeocharinus* sp.NHM RC/080; *13*, large proportion of articulated limb above opisthosoma of trigonotarbid, *P. scourfieldi* Hirst, 1923, NHM In 27756, *14*, detail of femur-patella articulation, *P. scourfieldi*, NHM In 27756; *15*, coxa of walking leg 2 and 3, showing trochanteral projection, *Palaeocharinus* sp. NHM RC/080; *16*, limb detail showing patella-tibia and tibia-metatarsus articulation, *P. scourfieldi*. NHM In 27756. Scale bars 1–9, 0.25 mm; 10, 0.1 mm; 11–16, 0.25 mm. Abbreviations: an=annulus; c1=coxa walking leg 1; c2=coxa walking leg 2; c-tr=coxa-trochanter articulation; ch=chelicera; cl=claw; en=endite; fe=femur; fe-pa=femur-patella articulation; gr=coxal granules; mt=metatarsus; pa=patella; pa-ti=patella-tibia articulation; pp=pedipalp; pr=trochanteral projection, op=opisthosoma; st=setae; ta=tarsus; ti=tibia; ti-mt=tibia-metatarsus articulation; tn=tendon; tr=trochanter; tr-fe=trochanter-femur articulation.

https://doi.org/10.1666/13-088 Published online by Cambridge University Press

original publication for full methods). To modify the mesh, the opisthosoma was selected: brush select (shortcut C), was used to highlight vertices at the posterior, ctrl + + enlarged the selection until the majority of opisthosomal vertices were selected, and then box select (B) was used to create a sharp anterior margin to the selection. Delete (X)→vertices removed these. The remaining prosoma was then remeshed (Properties panel→Object Modifiers→remesh, ocrtree depth 3, mode smooth, smooth shading). The reduced mesh was then modified manually to better match palaeocharinid morphology and create a more accurate reconstruction. The mesh was split along a sagittal plane, half was deleted, the clypeus was extended by selecting median vertices and dragging with high proportional editing falloff (PEF), and the lateral eye tubercle was moved posteriorly using a similar approach. Cones were created and added as spines on the clypeus (shift + A→mesh→cone) then scaled/modified using methods outlined in online Supplemental Data file 1. Median eyes were added (spheres, flattened) and positioned, as were lateral eye lenses. These were then united as a single mesh (ctrl + j), and a mirror modifier applied recreating the opposing half of the carapace. The two halves were then manually stitched to ensure a morphologically realistic join (by either merging vertices [alt + m] or joining them with an edge then a face [f]).

The opisthosoma was created in its entirety, through steps illustrated in Figure 2.1–2.5. This was required because no previously scanned trigonotarbids possess opisthosomal morphology similar to that observed in the Rhynie and Windyfield Chert paleocharinids. The opisthosoma was modeled on the basis of various cross-sectional morphologies observed in slides of the chert taxa: a cube was added, scaled to the correct proportions, and then modified with numerous loop cuts (Fig. 2.1). The anterior-posterior dorsal sutures were created with three closely spaced loop cuts, whereas each segment was created with two loop cuts, one significantly smaller than the other (Fig. 2.2). Further loop cuts were used to mold the ventral opisthosoma, and ensure the correct cross section (Fig. 2.3, 2.4). A subdivision surface modifier was added to smooth the morphology and make it appear more realistic (Catmull-Clark, 3 subdivisions; Fig. 2.5). Opisthosomal details such as the ventral sacs and pygidium were created from modified spheres and joined. The opisthosoma was then manually stitched to the prosoma. The mesh was then modified manually over several iterations to ensure good fit with the known morphology and published reconstructions of *Palaeocharinus* (e.g., Fayers et al., 2005, fig. 10). Opisthosomal muscle apodemes (dorsal depressions on each sternite) were created through the use of a boolean subtract modifier applied to the opisthosoma and a carefully positioned flattened sphere.

Limbs were created using similar methods to the opisthosoma (Fig. 2.6–2.11), based on the morphology observed in slides (Fig. 1), and the reconstructed articulations (Figs. 3, 4). Cylinders were created, a number of loop cuts (Fig. 2.6) were added, and their position were then adjusted (Fig. 2.7). Individual vertices were edited with PEF enabled to create the dorso-ventrally asymmetrical elements (Fig. 2.8). With the addition and editing of further loop cuts, and then application of a subdivision surface modifier (Fig. 2.9), limbs matching the morphology shown in Figure 1 were created. An armature was then created. These are used in Blender for rigging—they allow the user to create a control structure and then bind it to a mesh (skinning). When the armature, which consists of individual elements termed 'bones', is posed, it then deforms the mesh around it, allowing for more realistic and easier animation. A single 'bone' was added (shift + A→ armature→single bone), and then this was extruded (e) to create a series of seven connected 'bones' (six for the pedipalps) corresponding to the appropriate limb podomeres (Fig. 2.10). Each element was given a realistic constraint on the basis of the results reported below, i.e., fixed coxae, coxa-trochanter largely anterior-posterior and stiff, with trochanter-femur and femur-patella only allowing up and down movement, patella-tibia mobile with up and down movement and lateral rocking, tibia-metatarsus stiff with up down movement, metatarsus-tarsus mobile with limited up and down movement and lateral rocking. These were hard constraints in most cases, but on limbs with limited movement in a given direction (in contrast to none), the stiffness was instead increased to allow limited movement (found in bone tab of the properties window). For each limb reverse kinematics was applied (shift + I), with an empty (a Blender object which doesn't render) as a target allowing easy animation of both the distal limbs (via the empty) and the proximal podomeres (via the coxa) when walking. Limb is shown posed (Fig. 2.11). The limbs were then duplicated, resized as appropriate, and placed onto the model. Materials were applied to create color, and the armatures were parented to a central 'bone' to ease animation: this has the effect that the proximal limbs follow when the body advances. Subsequently, to allow for the 'alternating tetrapod' gait typically used by living spiders (e.g., Ward and Humphreys 1981; see discussion), the empties associated with the end of each of the limbs were parented to another empty, allowing each set of four limbs to be animated in unison for walking. Lights were added—four spots forming a square around the model with constant fall off and raytraced shadow, and anteriorly and posteriorly facing hemi lamps. A floor was placed in the scene (a plane) with a tiled appearance through a UV-mapped texture to show movement more clearly. A floor constraint was added to the distal-limb empties with the floor as a target, stopping the limbs from going through the plane. The animations were then keyframed using the timeline—for the walking gait this employed the empties associated with each quadruped. The graph editor was used to ensure realistic rates of movement between each keyframe. The forward movement for each step cycle was equal, and the floor was animated moving the same distance in the opposing direction. This allowed the walking animation to occur in place and obviate the need to move lighting. Once a single step cycle was successfully animated, this was replicated using the DopeSheet Summary. The camera location and rotation was then keyframed to create a video with a range of views of the trigonotarbid walking. For the flexing video, each leg was manually keyframed in pose mode of blender, and then rendered from four cameras at different angles. Four further spots were added for ventral illumination by duplicating the dorsal ones (shift + D).

RESULTS

Pedipalps.—Trigonotarbids possess pediform pedipalps, i.e., they are similar to the walking legs and lack raptorial projections for prey capture as in whip spiders (Amblypygi) or whip scorpions (Uropygi) or special organs for sperm transfer as in mature male spiders (Araneae). The trigonotarbid pedipalps are smaller than the adjacent legs and comprise six elements: coxa, trochanter, femur, patella, tibia and tarsus (Figs. 1.1, 1.4, 2; Dunlop, 1994b, pl. 8). The undivided tarsus bears a single claw (or pretarsus), later shown to be the movable finger of a small chelate structure in at least the Rhynie chert paleocharinids (Dunlop et al., 2009); similar to the condition in the pedipalp of the rare ricinuleids (Ricinulei). Articulations of the *Palaeocharinus* pedipalp (Fig. 3) based on Rhynie Chert material follow a format used by Shear et al. (1987) and Selden et al. (1991).

The palpal coxa in *Palaeocharinus* possesses four or five large, heavily sclerotized granules on its ventro-mesal surface and a setose mesal surface (Fig. 1.2, 1.5). It is unclear if the coxae were fixed or free to move. The articulation of the palpal coxa-

https://doi.org/10.1666/13-088 Published online by Cambridge University Press

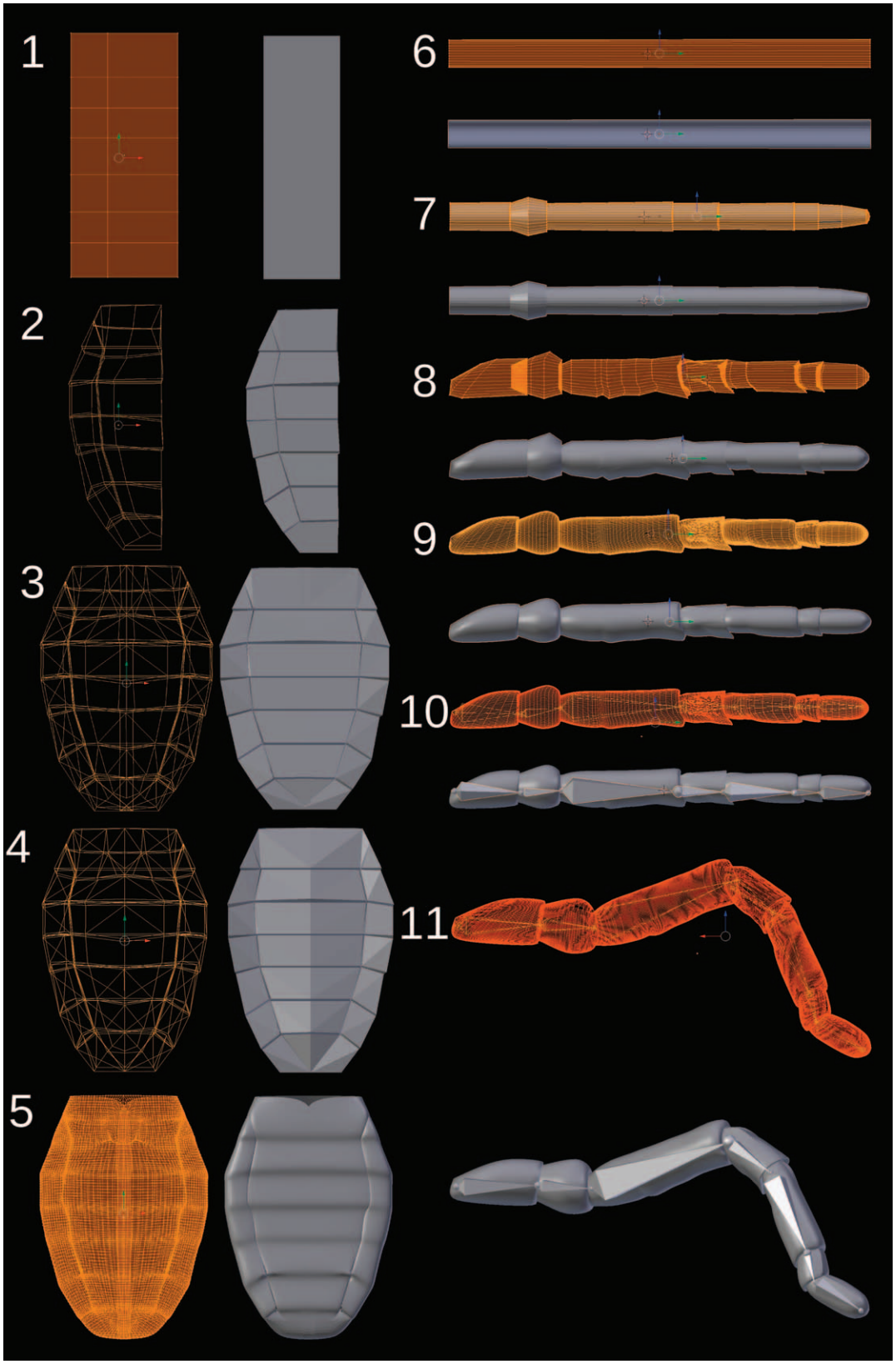

FIGURE 2—Box modeling procedure for the opisthosoma and limbs of the *Palaeocharinus* spp. model presented in Figure 6. Shown as both wireframe and solid meshes. *1–5*, the construction of the opisthosoma, modeled from a rectangle (*1*), through the addition of loop cuts (*2*), mirroring (*3*) and merging of the meshes (*4*), and then the application of a subsurface modifier (*5*); *6–11*, the construction and then rigging of the limbs; these were initially cylinders (*6*) to which loop cuts were added and resized (*7*); individual vertices were altered with PEF to create asymmetry (*8*), then a subsurface modifier was applied (*9*); subsequently an armature was created and applied (*10*) allowing the limbs to be posed (*11*).

https://doi.org/10.1666/13-088 Published online by Cambridge University Press

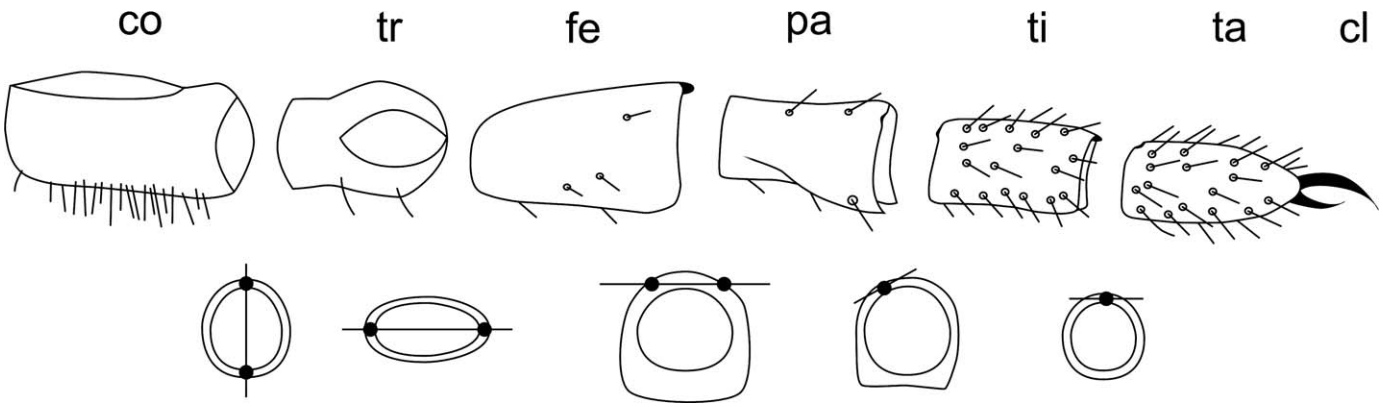

FIGURE 3—Articulations of the *Palaeocharinus* pedipalp based on Rhynie Chert material, with some details from Shear et al. (1987) and Dunlop et al. (2009). Schematic format follows that used by Shear et al. (1987) and Selden et al. (1991). Abbreviations: co=coxa; cl=claw; fe=femur; pa=patella; ta=tarsus; ti=tibia; tr=trochanter.

trochanter joint is equivocal in the fossils: analogy with spiders suggests movement in both the vertical and horizontal plane was possible. The trochanter-femur joint is an anterior-posterior, but obliquely angled articulation (NHM In 24671), and the femur is often the longest palpal podomere. The femur-patella joint is a superior bicondylar hinge (NHM In 27752, Dunlop, 1994b, pl. 44) and the patella is usually shorter than the femur. Its articulation with the tibia is a superior monocondylar hinge: NHM In 27752 and In 24673 suggest an articulation point slightly off-center (Fig. 1.4). This could mean that the distal podomere was orientated inwards in a slightly medial direction, but in general the pedipalp is not as well preserved as the legs in the Rhynie specimens and this interpretation should be treated with caution. The tibia-tarsus articulation of the palp is a superior monocondylar hinge (NHM In 27752, Dunlop, 1994b, pl. 44). The rounded distal termination of the pedipalp tarsus, with its chelate pretarsal claw and associated (?depressor) tendon of the movable claw finger was described in detail by Dunlop et al. (2009, fig. 3). A general reconstruction of the pedipalp in *Palaeocharinus* is presented (Fig. 3).

Walking legs.—Trigonotarbids have pediform walking legs composed of seven segments: coxa, trochanter, femur, patella, tibia, metatarsus and tarsus (Fig. 1.12). The latter are sometimes referred to as the basi- and telotarsus (cf. Shultz, 1989), given that this is an adesmatic or 'passive' joint in which the articulation between these elements lacks its own musculature, such that the metatarsus is thought to have simply divided off from the proximal end of the tarsus. Garwood and Dunlop (2011, text-fig. 2) suggested that trigonotarbids probably adopted the usual terrestrial arthropod 'hanging stance'; with an upward-pointing femur, a principal bend at the femur-patella joint, and then downward-pointing distal podomeres. Other fossils are often preserved in the typical arachnid 'death position', with the limbs folded tightly beneath the body and the distal podomeres straight. However, reconstructions of Carboniferous species such as *Eophrynus prestvicii* (Buckland, 1837) (Dunlop and Garwood, in press) inferred a more 'plantigrade' stance in life, i.e., the tarsus is bent outwards and placed somewhat flatter on the

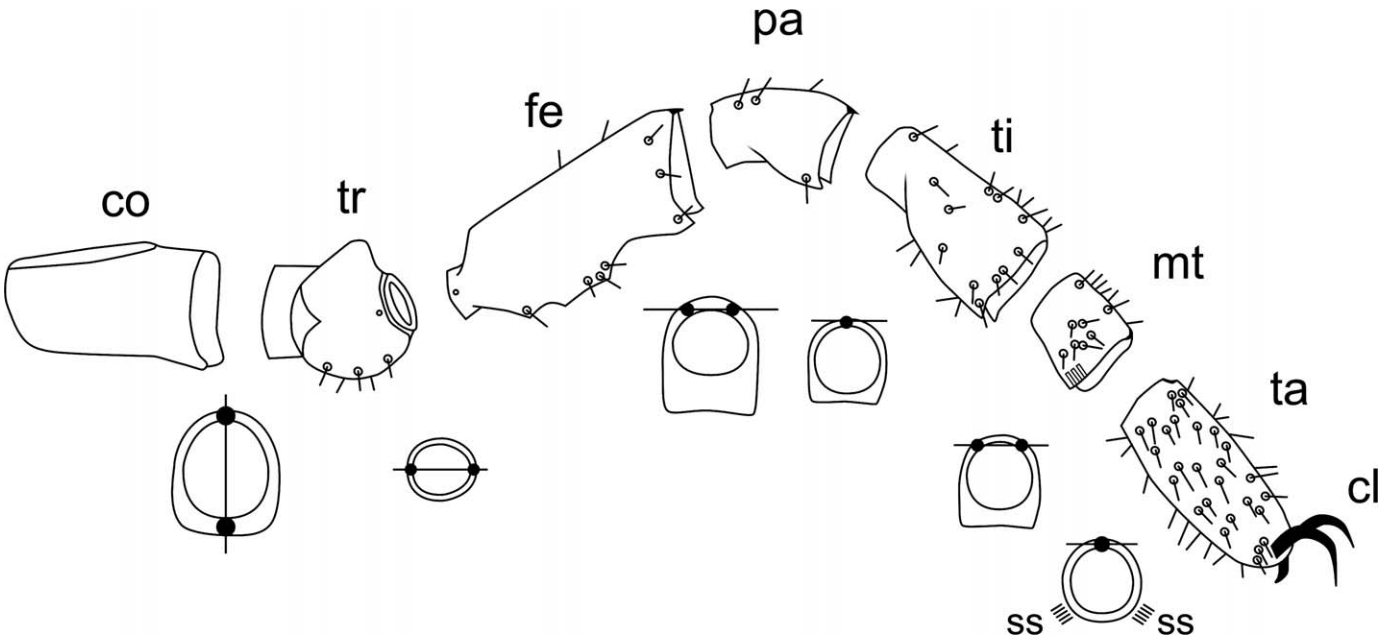

FIGURE 4—Articulations of the *Palaeocharinus* walking limb based on Rhynie Chert material. Schematic format follows that used by Shear et al. (1987) and Selden et al. (1991). Abbreviations: co=coxa; cl=claw; fe=femur; mt=metatarsus; pa=patella; ss=slit sensilla; ta=tarsus; ti=tibia; tr=trochanter.

https://doi.org/10.1666/13-088 Published online by Cambridge University Press

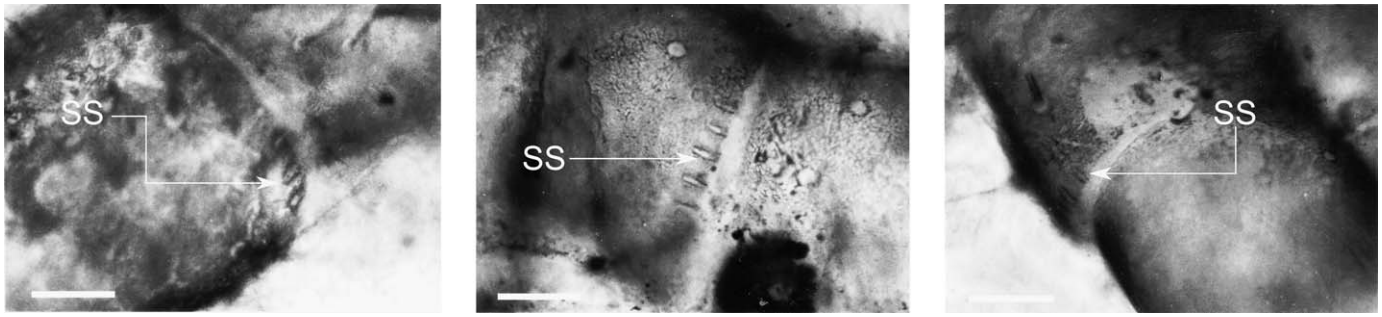

FIGURE 5—The lyriform slit sensilla (ss) found as two groups of six ventro-lateral slits parallel to the long axis of distal metatarsus. *1*, NHM specimen number In 27756; *2*, NHM specimen number In 27760; *3*, NHM specimen number In 27757. Scale bar=0.1 mm.

ground. This hypothesis is supported by comparisons with living arachnids, whereby the metatarsus may have separated off from the rest of the tarsus to allow the distal tip of the limb to flex outwards. Furthermore, the tarsal claws in the Rhynie Chert material (Fig. 1.8, 1.11) would be strongly displaced and risk breaking if a purely digitigrade stance was used. In general, the legs of trigonotarbids tend to be quite homogeneous and similar in robustness and length, although the fourth legs were usually longest, followed by the first, third and then second (i.e., a leg sequence of 4, 1, 3, 2 to use modern spider notation). There are a few exceptions, such as the family Anthracosironidae whose anterior legs are enlarged and raptorial. Leg four is often a little stouter than the rest. With the exception of the femur (see below), the limbs or trigontarbids exhibit little lateral flattening—they are largely rectangular to circular in cross-section (Fig. 1.7). A general reconstruction of the walking leg in *Palaeocharinus* is presented (Fig. 4).

The articulations reported here from the Rhynie Chert paleocharinids, differ in some aspects from those described by Shear et al. (1987) for trigonotarbids from the mid-Devonian of Gilboa. The leg coxae of *Palaeocharinus*, and some other trigonotarbids, possess mesal endites whose function remains unclear (Garwood et al., 2009; see Discussion). At present, there is no evidence for movable articulations at the body-coxae joint of the trigonotarbid walking legs. This is consistent with other arachnids, in which the coxae are largely fixed and the principal leg movement comes from the next articulation: the coxa-trochanter. Details of this joint are largely equivocal in *Palaeocharinus,* but in NHM In 24675 there are hints of at least a dorsal articulation point (Dunlop, 1994b) consistent with the infero-anterior and supero-posterior articulation points (Fig. 1.2) described in the Gilboa material (Shear et al., 1987). If correct, this would suggest a dorso-ventral bicondylar hinge. *Palaeocharinus* possesses spherical trochanters on legs one to three, in which there is a proximal projection which appears to slot into the coxa (Fig. 1.11,1.15). By contrast, trochanter four is larger and oval in shape. This pattern is seen in other trigonotarbid families, whose globose trochanters widen distally, and an oblique articulation to the femur aids the radiation of the legs. Distal to this, the trochanter-femur articulation (best seen in NHM In 24673) is clearly a horizontal anterior-posterior bicondylar hinge (Fig. 1.10, 1.11). It expresses a narrow ring of cuticle (the annulus), which encircles the trochanter-femur joint. The femur is usually the longest and broadest podomere and demonstrates a degree of lateral compression in some taxa.

The femur-patella joint is a superior bicondylar hinge, as seen in NHM In 24673 (Fig. 1.11) and In 27756 (Fig. 1.13, 1.14). Significantly, this joint lacks a ventral arcuate sclerite, an extra cuticular element embedded into the arthrodial membrane seen in spiders and the extinct and spider-like order Uraraneida (Selden et al., 1991, text-fig. 2). The *Palaeocharinus* patella is usually short and varies little between legs. The patella-tibia joint has a superior monocondylar hinge, clearly seen in NHM In 27756 (Fig. 1.13, 1.16) and In 24673 (Fig. 1.9, 1.11). Note that there is no corresponding ventral articulation point in *Palaeocharinus*, as is present in spiders (e.g., Clarke, 1986). In most trigonotarbid groups, the tibia is the second longest podomere and, in common with the femur, it is longer in legs 1 and 4. Towards the end of the limb the tibia-metatarsus joint is a superior bicondylar hinge, visible in NHM In 27756 (Fig. 1.16). In *Palaeocharinus* (and in anthracomartids) the metatarsus (or basitarsus in some terminologies) is short and almost quadratic; although this podomere is usually longer in other trigonotarbids. Study of *Palaeocharinus* also reveals almost lyriform groups of slit sensilla (Fig. 5): two groups of six slits parallel to the long axis of the podomere on the ventro-lateral distal metatarsus (NHM In 27756; see also Dunlop and Braddy, 1997, fig. 4). The metatarsus-tarsus joint is a superior monocondylar hinge (NHM In 27760, In 27758). The distal tarsus bears a dorsal tubercle from which a small number of relatively long setae emerge (Fig. 1.8), and a pair of large curved, pretarsal claws with a smaller, downward-pointing, medial, empodial claw (Fig. 1.11). These may have moved as a single unit, articulating against an antero-ventral pair of tarsal projections (NHM In 27758). A single (?claw depressor) tendon can clearly be seen running from the base of this claw unit (Fig. 1.8). Interestingly no corresponding levator tendon is visible, as would be predicted from the leg musculature of other arachnids (Shultz, 1989). If this tendon and muscle are genuinely absent, this could be interpreted as a putative trigonotarbid apomorphy and raises questions about how the claw unit was raised in life. Distal claws were presumably present in non-paleocharinid trigonotarbids too, but are only rarely preserved (e.g., Petrunkevitch, 1949, fig. 199) for anthracomartids.

Blender.—These results informed the limb motion of our Blender model, as outlined in the Blender methods section. Online Supplemental Data file 2 is a video, showing first the flexing of the limbs according to the articulations reported above, from a walking pose to under the body, and then back to their former position. Subsequently the video shows the likely walking gait for the trigonotarbids (see Discussion). Also presented are renders of the model (Fig. 6) at different stages of its walk cycle, with the center of mass (as estimated by Blender) marked. Blender files for both animations are provided as online Supplemental Data files 3 and 4.

DISCUSSION

Advantages and limitations of Blender, and comparisons to other software.—Blender is published under a GNU General Public License. It is both freely available and under regular development. Thus it has a number of strengths: it is free, and possesses diverse capabilities typical of high-end (normally

https://doi.org/10.1666/13-088 Published online by Cambridge University Press

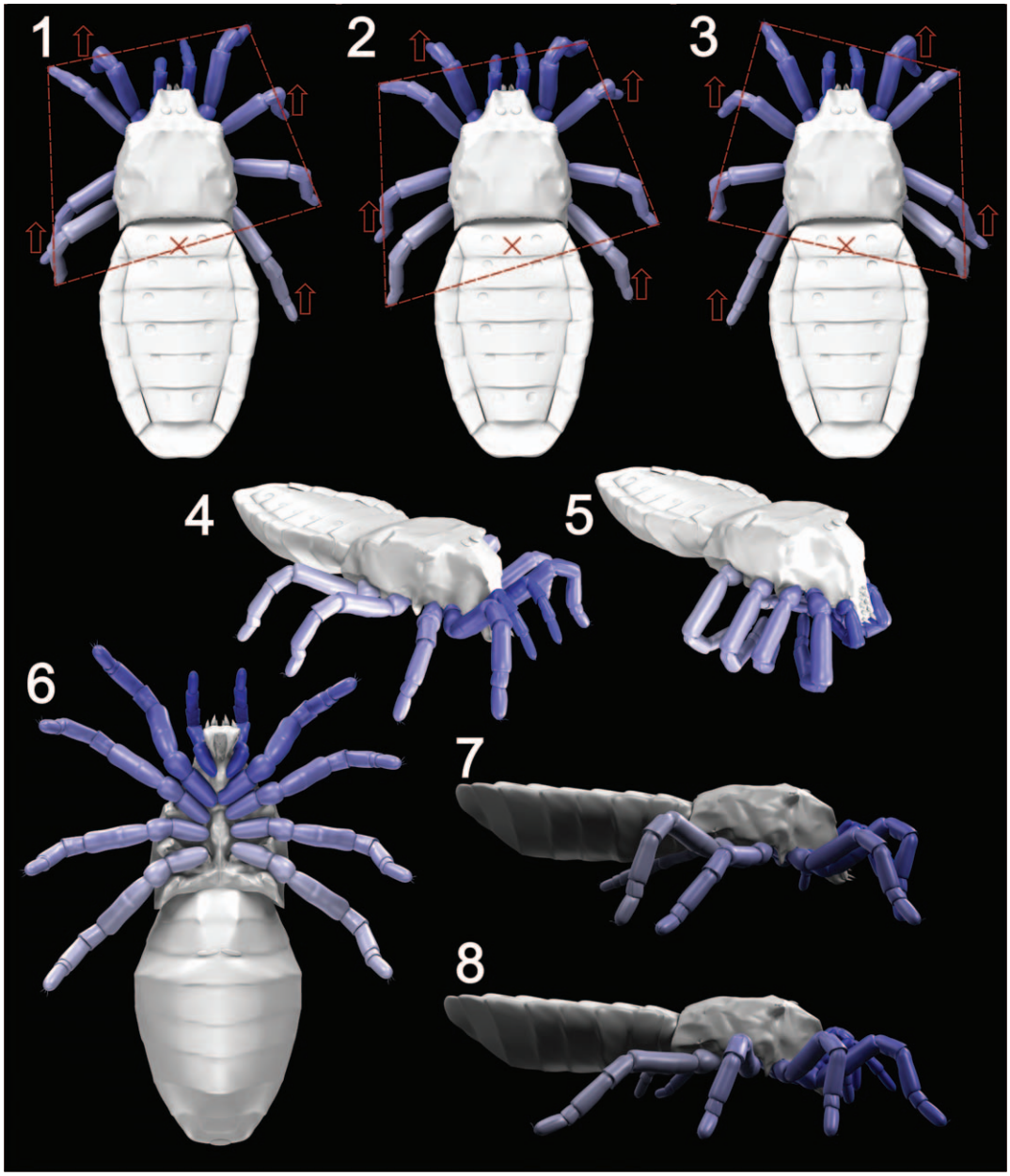

FIGURE 6—The *Palaeocharinus* spp. model created in Blender for the current study. *1–3*, different phases of the walking cycle from a dorsal perspective, with leg movements marked: *1*, *3*, opposing sets of four limbs are making contact with the floor; *2*, the midpoint between opposing steps in the cycle; limb motion is marked with arrows, the center of mass with a red cross, and a four-sided polygon defined by the four limbs in contact with the substrate is marked on with a dotted red line; this demonstrates that the center of mass remains within the line made by the legs on the ground at every point in the stepping cycle; *4*, an anterior-lateral view of the model with legs in a weight-bearing, plantigrade stance; *5*, the same view with legs curled beneath the body; *6*, ventral view; *7*, the step cycle from a lateral view, at equivalent to *2*; *8*, lateral view of the opposite part of the step cycle, mid-way between the position shown in *3* and *1*.

expensive) 3-D software. Furthermore, it is capable of importing/exporting a wide range of file formats, and modifying/animating meshes in many ways—accordingly, it can be useful in data processing, as well as rendering finalized images and movies.

There are, however, numerous limitations to the software: for the vast majority of virtual paleontology applications, it requires data which have been processed on other software prior to importing finalized meshes into Blender. Indeed, Blender is primarily a computer graphics package, and so allows the user almost unlimited freedom when creating and animating models. The software is not comparable to analytical software (e.g., SIMM; Hutchinson et al., 2005). Thus justification for anatomical and mechanical elements of Blender outputs—such as limb articulations and comparison with modern spiders in the current work—should be presented. Although it has improved considerably since Blender 2.4X, the Blender 2.5/2.6 graphical user interface (GUI), is custom-built, and is very different from a typical GUI, making it feel, at times, rather counterintuitive. As with any piece of 3-D software, especially one so versatile, there is also a steep learning curve (which this guide is intended to reduce). Nevertheless, many of the processing/creation capabilities of Blender can be found in other software, and the user needs to assess whether learning this program justifies the improvement achieved in rendered image quality. A strong user community (blender.org), and a number of books intended to introduce the software (Hess, 2010) are also helpful in this regard. Some

https://doi.org/10.1666/13-088 Published online by Cambridge University Press

datasets (CT in particular) tend to possess statistical noise (Sutton et al. 2013), which creates models with 'bumpy' surfaces, and thus very high triangle counts. In the current authors' experience, Blender universally loads these, however, manipulations and rendering can be slow with large models.

There are a number of three-dimensional computer animation suites comparable to Blender. These include 3ds Max, Autodesk Maya, ZBrush and Cinema 4D, to name a few, all of which differ subtly in their focus and capabilities. Of these Autodesk Maya (http://www.autodesk.com/products/autodesk-maya/overview) has arguably acquired the largest following in the paleontological community, albeit one which remains limited to a handful of researchers (Sellers et al., 2009; Molnar et al., 2012; Pittman et al., 2013). The software is available as a free 30-day trial (or, currently, a 3-yr free license for students), and the full package costs $3,675/£3,795. It differs from Blender in terms of its high end capabilities: both packages have individual features unavailable in the other. However, we believe that the capabilities of both extend far beyond the needs of the paleontological community. Thus one of the few advantages of Autodesk Maya is an arguably more intuitive user interface. However, for inexperienced users, the learning curve remains steep.

Animation.—Animating the Blender model required, in addition to the correct limb articulations outlined in the Results, an assessment of the likely gait. The walking legs of *Palaeocharinus* are fairly homogenous, all about the same length, and similar in shape and articulation to the legs of many spiders; particularly those with a free-living ecology such as tarantulas or wolf spiders, as opposed to web-builders which often have more elongate forelimbs and slender legs in general (see Foelix, 2011 for an overview). The most likely gait—also seen in other arachnids which employ an octopedal gait such as scorpions (Spagna and Peattie, 2012)—is thus an alternating tetrapod. Biancardi et al. (2011) demonstrated that the tarantula *Grammostola mollicoma*, employs two walking quadrupeds, with almost no phase delay between them (i.e., an almost ideal alternating tetrapod gait). The same gait is used at high speeds in fast-moving spiders but in a less rigid fashion. However, we should caution that variability is seen in many living taxa, both step-to-step and between step-cycles (Wilson, 1967; Ward and Humphreys, 1981; Spagna et al., 2011). For example, a tarantula walking slowly may move its legs one by one, in a somewhat wave-like sequence (JAD, personal observ.), and only switches to the more mechanical 'tetrapod' gait when running. Blender can display the center of mass of an object, which in this case lies on the opisthosomal macrotergite 2 + 3, about two-thirds from its anterior margin. This position is in agreement with the assumption that paleocharinids used an alternating tetrapod gait and Figure 6.1–6.3 demonstrate that throughout their walking cycle the center of mass would have remained within the quadruped in contact with the floor, therefore maintaining stability. For the videos presented herein (online Supplemental Data file 2) *Palaeocharinus* was made to walk fairly briskly with an idealized alternating tetrapod gait—and slight corresponding movements of the pedipalps—although in life a more variable and wave-like stepping pattern may have been adopted at low speeds.

Limb functional morphology.—Other than the distal claw, the pedipalps of *Palaeocharinus* show relatively few specializations and were probably used primarily for prey capture and/or the subsequent manipulation of food. The granular endites on the coxae might have played a role in mastication, similar to the serrated serrula seen on the palpal coxae ('maxillae' in some terminologies) of the more derived labidognath spiders (Foelix, 2011). In spiders these 'maxillae' are often quite mobile and can actively chew, but we can only speculate whether trigonotarbids also masticated prey using the pedipalpal coxae or simply pressed food items against the raised granules.

The legs of *Palaeocharinus* are generally better preserved and allow more inferences to be made. The extent of coxal mobility in life is hard to ascertain, but the projecting coxal endites in anthracomartids (Garwood et al., 2009) would only have allowed limited coxal movement, and the same was probably true of *Palaeocharinus* (e.g., Fayers et al., 2005). It is interesting to speculate whether the setose and granular mesal endites (Fig. 1.5) on at least the anterior leg coxae of *Palaeocharinus* are remnants of a gnathobase-like condition with (originally?) an active role in feeding. In a wider context, this may document an intermediate state in the shift from movable coxae with toothed gnathobases and an active role in food processing in an aquatic environment—as in the outgroups Xiphosura (horseshoe crabs) or Eurypterida (sea scorpions)—to the largely fixed coxae of most arachnids which form a solid, ventral base to the prosoma against which the rest of the legs can articulate when walking in the more biomechanically challenging conditions of a terrestrial environment.

Lack of coxal mobility implies that, as in Recent arachnids, the propulsive back stroke (remotor) and recovery forward stroke (promotor) action during walking derived primarily from the coxa-trochanter joint. The essentially dorso-ventral bicondylar hinge (Figs. 1.2, 4) inferred here would facilitate the anterior-posterior movement required to move the leg forwards. Note that in some extant arachnids, the coxa-trochanter joint is often more complex, and can also allow a degree of levator-depressor movement (cf. Shultz, 1989, 1999). Such freedom of movement is, in part, thanks to the presence of so-called intercalary sclerites (or a single sclerite in spiders) which have been reported from the coxa-trochanter articulation of the clade Tetrapulmonata (e.g., Shultz, 1990): a group comprising the spiders, whip spiders, whip scorpions and schizomids. Such sclerites have not been observed in any trigonotarbid to date, although their presence cannot be entirely ruled out. Drawing on the phylogenies of Shear et al. (1987) and Selden et al. (1991), Shultz (2007) recognized a Pantetrapulmonata clade comprising (Trigonotarbida + Tetrapulmonata). If intercalary sclerites are indeed absent in trigonotarbids this would imply 1) that these sclerites are apomorphic for Tetrapulmonata only and 2) that the trigonotarbid condition is plesiomorphic. Indeed a simple bicondylar articulation at this joint has been scored as plesiomorphic for arachnids (Shultz, 1990; Pepato et al., 2010). Furthermore, the apparent weakness of the articulation at this joint is coupled with a proximal projection slotting into the coxa in this joint (Fig. 1.15), reminiscent of a tubular 'ball and socket' joint. Both of these factors may indicate a relatively mobile articulation, albeit without strong condyles.

A strong, horizontal bicondylar hinge at the trochanter-femur joint suggests the principle levator-depressor movement of the leg probably originated here (Figs. 1.10, 4). The aforementioned annulus at this joint—a cuticular ring seen in both the Rhynie and Gilboa paleocharinids (Shear et al., 1987)—may have strengthened the narrow proximal region of the femur. The presence of an annulus in non-Devonian trigonotarbids remains equivocal. Note that sclerites in this joint membrane are seen in both modern and fossil Amblypygi (Dunlop and Martill, 2002) and the annulus could be homologous with these sclerites given that trigonotarbids usually resolve basal to the tetrapulmonates (see above). This annulus has been compared to the 'double trochanter' or 'divided femur' in other arachnids, but the polarity of this character state remains poorly understood; see Shultz (1989, 2007) for further discussion of homology and the hypothesis of a separate basi- and telofemur in the arachnid ground pattern.

While strong, the femur-patella joint in *Palaeocharinus* was likely to have had a lower degree of flexion than is possible at the same 'knee' joint in spiders. The arcuate sclerite on the underside

of this joint in spiders permits more extreme flexion by providing a muscle attachment site allowing the animals to pull the leg in further and more tightly. The patella-tibia articulation in *Palaeocharinus* is a superior monocondylar joint (Fig. 1.9, 1.16), lacking a ventral articulation point corresponding to the dorsal one, and thus allowing the joint freedom of movement both dorso-ventrally and, to some extent, laterally. It could thus have acted as a 'rocking joint', homologous to that observed in spiders, which has been interpreted as an adaptation for preventing tarsal abrasion by allowing the leg to twist during walking (Manton, 1977). If true, it would also offer stability to the animal and act as a form of suspension system, allowing forces generated in the legs to be isolated from the body. It is worth noting that in spiders with a fully developed rocking joint, the ventral condyle at the patella-tibia joint, which appears to be absent in *Palaeocharinus*, is often less well-developed than the dorsal one (Clarke, 1986), and is coupled with a compression zone of cuticle (Manton, 1977). It is unlikely, however, that the freedom of lateral movement for the patella-tibia joint in trigonotarbids was similar to that of spiders due to a lack of morphological modification on the lateral margins of either the patella or tibia at this joint. Furthermore, the joint lacks extensive lateral arthrodial membranes. Though musculature is poorly known, the joint may have demonstrated primarily levator-depressor movement, with some lateral movement of the distal podomeres of the leg permitted by the joint's monocondylar nature. Proximal rocking could thus have been facilitated by the relatively mobile coxa-trochanter joint, with counter-rocking at the metatarsus-tarsus joint to create a passive rocking system.

The fact that the tibia-metatarsus joint in *Palaeocharinus* is a simple superior bicondylar hinge (Figs. 1.16, 4) suggests it was restricted to levator-depressor movement only, and a lack of extensive arthrodial membrane probably precluded a high degree of freedom. The metatarsus-tarsus articulation is herein reported as a superior monocondylar hinge (Fig. 1.3, 1.8) in *Palaeocharinus*. This is in contrast to the bicondylar hinge reported in Gilboa taxa by Shear et al. (1987). In *Palaeocharinus* the monocondylar joint may have allowed counter-rocking movement, as reported for the spider metatarsus-tarsus (cf. Manton, 1977). However, lack of modification to the lateral podomere margins at this articulation and the poorly developed lateral arthrodial membrane implies a restricted degree of lateral movement. The joint also lacks an extensive ventral arthrodial membrane, suggesting little dorso-ventral flexibility. Combined with a superior articulation point, this would have precluded *Palaeocharinus* from placing the tarsus flat on the substrate in a fully plantigrade stance. Note that Clarke (1986) reported a strengthened arthrodial membrane at this joint in spiders. If this were true for the Rhynie fossils, it would mean that the ventral membrane could compensate for the stresses of an outwardly directed tarsus articulating from the dorsal monocondylar hinge.

Proprioceptors.—Proprioception towards the end of the limbs was probably important for trigonotarbids when walking, especially when traversing an irregular leaf litter substrate in the early forest ecosystems. Slit sensilla, which act as cuticular 'strain gauges' (Barth, 1985, 2012), are found on the metatarsus, and may have helped in this regard. These could detect cuticular strains perpendicular to the long axis of the leg and thus may have provided sensory information about the degree of loading of the metatarsus-tarsus joint. This could also have aided the rocking mechanism of the leg, allowing *Palaeocharinus* to determine the direction and magnitude of the rocking motion, and sense lateral displacement of the tarsus due to obstacles during locomotion. It is interesting to note that in *Palaeocharinus* slit sensilla are only found on the metatarsus, which raises the question whether these proprioceptors first evolved at this adesmatic leg joint which had no musculature of its own to provide sensory feedback about, for example, joint loading. It is possible that slit sensilla subsequently spread out over the rest of the cuticle to provide sensory data at the other eudesmatic (i.e., muscle-bearing) articulation points.

CONCLUSION

Blender is a freely available, open-source, and versatile piece of software, which can be of great utility to paleontologists who need to present the results of their work in three-dimensions. It does, however, have a steep learning curve, and accordingly its benefits should be weighed against the necessary time investment for any given project. It is hoped the guide in online Supplemental Data file 1 and this contribution are helpful in introducing the basics of the software to new scientific users. As an example, we reconstructed here the limb articulations of one of the first terrestrial predators, and our results and interpretations are summarized in the final Blender animation. In addition to its scientific value, this offers further possibilities for outreach and public engagement in science through bringing a long-dead animal 'back to life' (see also Rahman et al., 2012). Our data suggest that these extinct trigonotarbid arachnids probably flexed their legs and walked in a similar fashion to modern cursorial spiders. That said, it is important to stress that the *Palaeocharinus* limb appears not to possess certain innovations seen in more derived arachnids, namely: 1) intercalary sclerites associated with the coxa; 2) an arcuate sclerite at the femur-patella joint; 3) bicondylar patella-tibia 'rocking joints'; 4) a long metatarsus; and thus 5) a fully plantigrade tarsus. These extinct arachnids may thus have lacked some of the sophistication seen in the walking behavior of modern spiders. Yet trigonotarbids offer a useful starting point for investigating how ancient arthropods adapted their limbs for locomotion after first emerging onto land.

ACKNOWLEDGMENTS

We would like to thank all involved in the Blender Foundation and community for providing their skill, knowledge, coding and software for free; C. Mellish and M. Munt (NHM) for access to specimens in their care; G. Edgecombe for the loan of his microscope; S. Lautenschlager and M. Poschmann for constructive reviews; and I. Rahman and S. Smith for their support by inviting this submission. RG would like to thank J. T. Haug for his 2007 recommendation to experiment with Blender. RG is an 1851 Royal Commission Research Fellow and a Scientific Associate at the NHM.

ACCESSIBILITY OF SUPPLEMENTAL DATA

Supplemental data deposited in Dryad repository: http://dx.doi.org/10.5061/dryad.1v2s7.

REFERENCES

Abel, R. L., C. Laurini, and M. Richter. 2012. A palaeobiologist's guide to "virtual" micro-CT preparation. Palaeontologia Electronica, 15:6T, 17 p.

Arvo, J. R. 1986. Backward ray tracing. Developments in Ray Tracing, SIGGRAPH '86, 12:259–263.

Barth, F. G. 1985. Slit sensilla and the measurement of cuticular strains, p. 162–188. *In* Neurobiology of Arachnids. Springer-Verlag, New York.

Barth, F. 2012. Strain and substrate motion: spider strain detection; p. 251–273. *In* F. G. Barth, J. A. C. Humphrey, and M. V. Srinivasan (eds.), Frontiers in Sensing. Springer.

Bercovici, A., A. Hadley, and U. Villanueva-Amadoz. 2009. Improving depth of field resolution for palynological photomicrography. Palaeontologia Electronica, 12, 12 p.

Biancardi, C. M., C. G. Fabrica, P. Polero, J. F. Loss, and A. E. Minetti. 2011. Biomechanics of octopedal locomotion: kinematic and kinetic analysis of the spider *Grammostola mollicoma*. The Journal of Experimental Biology, 214:3,433–3,442.

BUCKLAND, W. 1837. The Bridgewater Treatises on the Power, Wisdom, and Goodness of God, as Manifested in the Creation. Treatise VI: Geology and Mineralogy Considered with Reference to Natural Theology. William Pickering, London, 143 p.

CLARIDGE, M. F. AND A. G. LYON. 1961. Lung-books in the Devonian Palaeocharinidae (Arachnida). Nature, 191:1,190–1,191.

CLARKE, J. 1986. The comparative functional morphology of the leg joints and muscles of five spiders. Bulletin of the British Arachnological Society, 7: 37–47.

COOK, R. L., T. PORTER, AND L. CARPENTER. 1984. Distributed Ray Tracing. Computer Graphics, 18:137–145.

DUNLOP, J. A. 1994a. Filtration mechanisms in the mouthparts of tetrapulmonate arachnids (Trigonotarbida, Araneae, Amblypygi, Uropygi, Schizomida). Bulletin of the British Arachnological Society, 9:267–273.

DUNLOP, J. A. 1994b. Palaeobiology of the Trigonotarbida. Ph.D. Thesis, University of Manchester, 614 p.

DUNLOP, J. A. 1996. A trigonotarbid arachnid from the Silurian of Ludford Lane, Shropshire. Palaeontology, 39:605–614.

DUNLOP, J. A. AND S. J. BRADDY. 1997. Slit-like structures on the prosomal appendages of the eurypterid *Baltoeurypterus*. Neues Jahrbuch für Geologie und Paläontologie, Monatshefte, 1997:31–38.

DUNLOP, J. A. AND R. J. GARWOOD. In press. Tomographic reconstruction of the exceptionally preserved trigonotarbid arachnid *Eophrynus prestvicii*. Acta Palaeontologica Polonica.

DUNLOP, J. A. AND D. M. MARTILL. 2002. The first whipspider (Arachnida: Amblypygi) and three new whipscorpions (Arachnida: Thelyphonida) from the Lower Cretaceous Crato Formation of Brazil. Transactions of the Royal Society of Edinburgh, Earth Sciences, 92:325–334.

DUNLOP, J. A. AND R. RÖßLER. 2013. The youngest trigonotarbid, from the Permian of Chemnitz in Germany. Fossil Record, 16:229–243.

DUNLOP, J. A. AND P. A. SELDEN. 2004. A trigonotarbid arachnid from the Lower Devonian of Tredomen, Wales. Palaeontology, 47:1,469–1,476.

DUNLOP, J. A., C. KAMENZ, AND G. TALARICO. 2009. A fossil trigonotarbid arachnid with a ricinuleid-like pedipalpal claw. Zoomorphology, 128:305–313.

FAYERS, S. R. AND N. H. TREWIN. 2004. A review of the palaeoenvironments and biota of the Windyfield chert. Transactions of the Royal Society of Edinburgh, Earth Sciences, 94:325–339.

FAYERS, S. R., J. A. DUNLOP, AND N. H. TREWIN. 2005. A new Early Devonian trigonotarbid arachnid from the Windyfield Chert, Rhynie, Scotland. Journal of Systematic Palaeontology, 2:269–284.

FOELIX, R. 2011. Biology of Spiders, third edition. Oxford University Press, Oxford, viii + 419 p.

FRIČ, A. 1904. Palaeozoische Arachniden. Privately published with support from the Imperial Academy, Vienna. Dr. Eduard Grégr, Prague, 80 p.

GARWOOD, R. J. AND J. A. DUNLOP. 2011. Morphology and systematics of Anthracomartidae (Arachnida: Trigonotarbida). Palaeontology, 54:145–161.

GARWOOD, R. J., J. A. DUNLOP, G. GIRIBET, AND M. D. SUTTON. 2011. Anatomically modern Carboniferous harvestmen demonstrate early cladogenesis and stasis in Opiliones. Nature Communications, 2:444.

GARWOOD, R. J., J. A. DUNLOP, AND M. D. SUTTON. 2009. High-fidelity X-ray micro-tomography reconstruction of siderite-hosted Carboniferous arachnids. Biology Letters, 5:841–844.

GARWOOD, R. J., I. A. RAHMAN, AND M. D. SUTTON. 2010. From clergymen to computers—the advent of virtual palaeontology. Geology Today, 26:96–100.

GARWOOD, R. J., A. ROSS, D. SOTTY, D. CHABARD, S. CHARBONNIER, M. D. SUTTON, AND P. J. WITHERS. 2012. Tomographic Reconstruction of Neopterous Carboniferous Insect Nymphs. PLoS ONE, 7:e45779.

GARWOOD, R. J. AND M. D. SUTTON. 2010. X-ray micro-tomography of Carboniferous stem-Dictyoptera: new insights into early insects. Biology Letters, 6:699–702.

GARWOOD, R. J. AND M. D. SUTTON. 2012. The enigmatic arthropod *Camptophyllia*. Palaeontologia Electronica, 15, 12 p.

GILES, S. AND M. FRIEDMAN. 2013. Virtual reconstruction of brain anatomy in early ray-finned fishes (Osteichthyes: Actinopterygii). Journal of Palaeontology, 88:636–651.

HAUG, J. T. AND C. HAUG. 2012. An unusual fossil larva, the ontogeny of achelatan lobsters, and the evolution of metamorphosis. Bulletin of Geosciences, 88:195–206.

HAUG, J. T., A. MAAS, C. HAUG, AND D. WALOSZEK. 2011. *Sarotrocercus oblitus*–small arthropod with great impact on the understanding of arthropod evolution? Bulletin of Geosciences, 86:725–736.

HAUG, J. T., D. WALOSZEK, A. MAAS, Y. LIU, AND C. HAUG. 2012. Functional morphology, ontogeny and evolution of mantis shrimp-like predators in the Cambrian. Palaeontology, 55:369–399.

HESS, R. 2010. The Essential Guide to Learning Blender 2.6. Focal Press, London, UK, 416 p.

HIRST, S. 1923. On some arachnid remains from the Old Red Sandstone. Annals and Magazine of Natural History, 12:455–474.

HIRST, S. AND S. MAULIK. 1926. On some arthropod remains from the Rhynie chert (Old Red Sandstone). Geological Magazine, 63:69–71.

HUTCHINSON, J. R., F. C. ANDERSON, S. S. BLEMKER, AND S. L. DELP. 2005. Analysis of hindlimb muscle moment arms in *Tyrannosaurus rex* using a three-dimensional musculoskeletal computer model: implications for stance, gait, and speed. Palaeobiology 31:676–701.

HYŽNÝ, M., Š. JÓZSA, J. A. DUNLOP, AND P. A. SELDEN. 2013. A fossil arachnid from Slovakia: the Carboniferous trigonotarbid *Anthracomartus voelkelianus* Karsch, 1882. Arachnology, 16:21–26.

KAMENZ, C., J. A. DUNLOP, G. SCHOLTZ, H. KERP, AND H. HASS. 2008. Microanatomy of Early Devonian book lungs. Biology Letters, 4:212–215.

MANTON, S. M. 1977. The Arthropoda: Habits, Functional Morphology, and Evolution. Clarendon Press, Oxford, 527 p.

MOLNAR, J. L., S. E. PIERCE, J. A. CLACK, AND J. R. HUTCHINSON. 2012. Idealized landmark-based geometric reconstructions of poorly preserved fossil material: a case study of an early tetrapod vertebra. Palaeontologia Electronica, 15:1–18.

PARRY, S. F., S. R. NOBLE, Q. G. CROWLEY, AND C. H. WELLMAN. 2011. A high-precision U–Pb age constraint on the Rhynie Chert Konservat-Lagerstätte: time scale and other implications. Journal of the Geological Society, London, 168:863–872.

PEPATO, A. R., C. E. F. ROCHA, AND J. A. DUNLOP. 2010. Phylogenetic position of the acariform mites: sensitivity to homology assessment under total evidence. BMC Evolutionary Biology, 10:1–23.

PETRUNKEVITCH, A. I. 1949. A study of Palaeozoic Arachnida. Transactions of the Connecticut Academy of Arts and Sciences, 37:69–315.

PETRUNKEVITCH, A. I. 1953. Paleozoic and Mesozoic Arachnida of Europe. Geological Society of America, Memoir 53, Boulder, 128 p.

PITTMAN, M., S. M. GATESY, P. UPCHURCH, A. GOSWAMI, AND J. R. HUTCHINSON. 2013. Shake a tail feather: the evolution of the theropod tail into a stiff aerodynamic surface. PLoS ONE, 8:e63115.

POCOCK, R. I. 1911. A monograph of the terrestrial Carboniferous Arachnida of Great Britain. Monographs of the Palaeontographical Society, 64:1–84.

POSCHMANN, M. AND J. A. DUNLOP. 2010. Trigonotarbid arachnids from the Lower Devonian (lower Emsian) of Alken an der Mosel (Rhineland-Palatinate, SW Germany). Paläontologische Zeitschrift, 84:467–484.

POSCHMANN, M. AND J. A. DUNLOP. 2011. Trigonotarbid arachnids from the Lower Devonian (Siegenian) of Bürdenbach (Lahrbach Valley, Westerwald area, Rhenish Slate Mountains, Germany). Paläontologische Zeitschrift, 85: 433–447.

RAHMAN, I. A., K. ADCOCK, AND R. J. GARWOOD. 2012. Virtual fossils: a new resource for science communication in paleontology. Evolution: Education and Outreach, 5:635–641.

RICE, C. M., N. H. TREWIN, AND L. I. ANDERSON. 2002. Geological setting of the Early Devonian Rhynie cherts, Aberdeenshire, Scotland: an early terrestrial hot spring system. Journal of the Geological Society, 159:203–214.

SELDEN, P. A., W. A. SHEAR, AND P. M. BONAMO. 1991. A spider and other arachnids from the Devonian of New York, and reinterpretations of Devonian Araneae. Palaeontology, 34:241–281.

SELLERS, W. I., P. L. MANNING, T. LYSON, K. STEVENS, AND L. MARGETTS. 2009. Virtual palaeontology: gait reconstruction of extinct vertebrates using high performance computing. Palaeontologia Electronica, 12:11–26.

SHEAR, W. A. 2000. *Gigantocharinus szatmaryi*, a new trigonotarbid arachnid from the Late Devonian of North America (Chelicerata: Arachnida: Trigonotarbida). Journal of Paleontology, 74:25–31.

SHEAR, W. A., P. A. SELDEN, W. D. I. ROLFE, P. M. BONAMO, AND J. D. GRIERSON. 1987. New terrestrial arachnids from the Devonian of Gilboa, New York (Arachnida: Trigonotarbida). American Museum Novitates, 2901:1–74.

SHULTZ, J. W. 1987. Walking and surface film locomotion in terrestrial and semi-aquatic spiders. Journal of Experimental Biology, 444:427–444.

SHULTZ, J. W. 1989. Morphology of locomotor appendages in Arachnida: evolutionary trends and phylogenetic implications. Zoological Journal of the Linnean Society, 97:1–55.

SHULTZ, J. W. 1990. Evolutionary morphology and phylogeny of Arachnida. Cladistics, 6:1–38.

SHULTZ, J. W. 1999. Muscular anatomy of a whipspider, *Phrynus longipes* (Pocock) (Arachnida: Amblypygi), and its evolutionary significance. Zoological Journal of the Linnean Society, 126:81–116.

SHULTZ, J. W. 2007. A phylogenetic analysis of the arachnid orders based on morphological characters. Zoological Journal of the Linnean Society, 150: 221–265.

SPAGNA, J. C. AND A. M. PEATTIE. 2012. Terrestrial locomotion in arachnids. Journal of Insect Physiology, 58:599–606.

SPAGNA, J. C., E. A. VALDIVIA, AND V. MOHAN. 2011. Gait characteristics of two fast-running spider species (*Hololena adnexa* and *Hololena curta*), including an aerial phase (Araneae: Agelenidae). Journal of Arachnology, 39:84–91.

SPENCER, A. R. T., J. HILTON, AND M. D. SUTTON. 2012. Combined methodologies for three-dimensional reconstruction of fossil plants preserved in siderite nodules: *Stephanospermum braidwoodensis* nov. sp. (Medullosales) from the Mazon Creek lagerstätte. Review of Palaeobotany and Palynology, 188:1–17.

STEIN, M. 2010. A new arthropod from the early Cambrian of North Greenland, with a "great appendage"-like antennula. Zoological Journal of the Linnean Society, 158:477–500.

STEIN, M. AND P. A. SELDEN. 2012. A restudy of the Burgess Shale (Cambrian) *arthropod Emeraldella brocki* and reassessment of its affinities. Journal of Systematic Palaeontology, 10:361–383.

SUTTON, M. D. 2008. Tomographic techniques for the study of exceptionally preserved fossils. Proceedings of the Royal Society of London, Series B, Biological Sciences, 275:1,587–1,593.

SUTTON, M. D., R. J. GARWOOD, D. J. SIVETER, AND D. J. SIVETER. 2012. Spiers and VAXML: a software toolkit for tomographic visualisation, and a format for virtual specimen interchange. Palaeontologia Electronica, 15, 14 p.

SUTTON, M. D., I. A. RAHMAN, AND R. J. GARWOOD. 2013. Techniques for Virtual Palaeontology. Wiley-Blackwell, 208 p.

WARD, T. M. AND W. F. HUMPHREYS. 1981. Locomotion in burrowing and vagrant wolf spiders (Lycosidae). Journal of Experimental Biology, 92: 305–321.

WHITTED, T. 1980. An improved illumination model for shaded display. Graphics and Image Processing, 23:343–349.

WILSON, D. M. 1967. Stepping patterns in tarantula spiders. Journal of Experimental Biology, 47:133–151.

ZAMORA, S., I. A. RAHMAN, AND A. B. SMITH. 2012. Plated Cambrian bilaterians reveal the earliest stages of echinoderm evolution. PLoS ONE, 7:e38296.

ACCEPTED 1 OCTOBER 2013